Available online at www.sciencedirect.com
SCIENCE DIRECT®
Journal of Solid State Chemistry 171 (2003) 262–267
JOURNAL OF SOLID STATE CHEMISTRY
http://elsevier.com/locate/jssc

Crystal-field analysis of Eu^{3+} energy levels in the new rare-earth *R* $BiY_{1-x}R_xGeO_5$ oxide

C. Cascales* and C. Zaldo

Instituto de Ciencia de Materiales de Madrid, CSIC, Campus de Cantoblanco, Madrid E-28049, Spain

Received 27 May 2002; received in revised form 1 August 2002; accepted 21 August 2002

Abstract

Pale colored $BiY_{1-x}R_xGeO_5$ (*R* = rare-earth from Pr to Yb) polycrystalline samples exhibit a crystalline phase isostructural with the orthorhombic *Pbca* (No. 61) structure-type established for $BiYGeO_5$ and $BiYbGeO_5$. *R* occupies a single point site in the host, with the lowest C_1 symmetry. While for Pr and Nd *x* must be $\leqslant 0.35$, for smaller *R* ions, Sm to Yb, the phase appears for any *x* content. Detailed crystallographic data for $BiErGeO_5$ have been determined from the structure refinement of its neutron diffraction profile at room temperature. Optical absorption and photoluminescence measurements at 10 K have been performed for $BiEuGeO_5$. An initial approach to the parametrization of crystal-field effects on this new host has been provided by results of the semi-empirical Simple Overlap Model, which considers the crystallographic positions of the nearest neighbors around *R*. Furthermore, the strongly reduced $^7F_{JM}$ set of levels of the $4f^6$ configuration has been taken into account for a trustworthy phenomenological determination of crystal-field parameters of the observed optical center for the Eu^{3+} sample. In spite of difficulties imposed by the low symmetry of Eu^{3+}, a very good root mean squares deviation $\sigma = 5.6\,cm^{-1}$ between experimental and simulated energy level schemes has been obtained considering the approximate $C_2(C_s)$ symmetry for the Eu^{3+} in the host.

Keywords: Rare-earth germanates; $6s^2$-Bi(III) non-bonding pair; Spectroscopic properties of Eu^{3+}; Crystal-field analysis

1. Introduction

The existence of a new family of germanates with formula $BiRGeO_5$ has been recently reported [1]. The simultaneous presence of Bi^{3+}, which possesses a non-bonding $6s^2$ electron pair, and a trivalent rare-earth ion *R*, is likely to lead to interesting properties in these compounds. The structure solved on single crystals of both Y and Yb phases is orthorhombic, space group *Pbca* (No. 61). These materials can be considered intermediate terms in the $Bi_{2-a}R_aGeO_5$ ($0 \leqslant a \leqslant 2$) general series, with Bi_2GeO_5 ($a = 0$) [2–4] and R_2GeO_5 ($a = 2$) [5–7] as limit phases. With regards to the also orthorhombic $Cmc2_1$ Bi_2GeO_5 [2], the new packing appears as a consequence of the formation of $(RO_7)_6$ units in the ac $(GeRO_5)_\infty$ layers, which forces the reorganization of Bi and Ge polyhedra doubling the unit-cell of Bi_2GeO_5. In the end of the series, R_2GeO_5 ($a = 2$), very different structures appear, depending on the *R* size.

To investigate the potentialities of this structure as a host for solid state laser technology, we are carrying out a complete collection of room temperature and 10 K optical absorption OA and photoluminescence PL measurements for rare-earths *R*, from Pr to Yb. The derived data will be firstly used to examine their crystal-field (CF) interactions at the *R* site. It is well known that in the initial determination of *the number* of non-equivalent optical centers in the host (also the existence of other than the expected crystalline phase in a powdered sample) as well as for the assignment of the irreducible representation of the ground crystal-field level, is very helpful to consider transitions from the ground level to a non-degenerate excited state. Examples are the $^3P_0$, $^2P_{1/2}$ and $^5D_0$ energy levels of Pr^{3+}, Nd^{3+} and Eu^{3+} ions, respectively. The later configuration, as an even electron system, is also suitable as probe for *the site symmetry*, since on the basis of the observed *J* splittings it can be deduced quite straightforwardly. Furthermore, other especial characteristics of the $4f^6$

*Corresponding author. Fax: +34-91-372-0623.
E-mail addresses: ccascales@icmm.csic.es (C. Cascales), cezaldo@icmm.csic.es (C. Zaldo).

0022-4596/03/$ - see front matter © 2003 Elsevier Science (USA). All rights reserved.
doi:10.1016/S0022-4596(02)00173-1

configuration, explained below, confirm Eu^{3+} as the best choice for a 'crystal-field probe'.

The work reported here describes the conditions of the synthesis of stoichiometric and *R*-doped $BiY_{1-x}R_xGeO_5$ germanates, the refinement of the crystal structure of a selected member of the series, $BiErGeO_5$, from neutron powder diffraction NPD data, and the crystal-field simulation of the observed Eu^{3+} energy levels in the host. The phenomenological calculation of CF effects has been carried out using the single-particle CF theory, and conducted on the basis of the strongly reduced $^7F_{JM}$ set alone [8], i.e. only considering 49 $|SLJM_J\rangle$ levels. A descending symmetry method [9], from approximate C_{2v} to $C_2(C_s)$ point symmetries, has been used in the fitting procedure. The same simulation was performed with CF parameters from the semi-empirical Simple Overlap Model (SOM) [10], considering in this case the R^{3+} real point symmetry, C_1. Together with adequate free-ion parameters, phenomenological CF parameters obtained for Eu^{3+} will constitute a convenient set of starting values in the simulation of the energy level schemes and expressions of the associated wavefunctions for the remaining $4f^N$ configurations.

2. Structural background

The family of $BiY_{1-x}R_xGeO_5$, R = Pr to Yb, compounds exhibits a crystalline phase isostructural with the orthorhombic *Pbca* (No. 61) structure-type established for $BiYGeO_5$ and $BiYbGeO_5$ [1]. The structure is formed by $(GeRO_5)_\infty$ layers containing both $(RO_7)_6$-units of edge sharing RO_7 polyhedra, defined as C_{2v}-monocapped trigonal prisms, and GeO_4 tetrahedra, as depicted in Fig. 1. *R* occupies a single point site in the host, with the lowest C_1 symmetry. Between these layers zigzag chains of ψ-BiO_5 octahedra are running in the *a* direction. The stereoelectronic effect of the Bi^{3+} lone pair, that is pointing out to the sixth vertex of the octahedron, leads to this apparent zigzag, and therefore to the kind of packing in this new structure type.

3. Experimental details

Polycrystalline samples of $BiY_{1-x}R_xGeO_5$ (R = Pr to Yb) were prepared in zirconia crucibles, LECO 528–018, from mixtures of reagent grade Bi_2O_3, Y_2O_3, R_2O_3 and GeO_2. The mixtures were ground, heated in air at successive temperatures of 1073, 1173 and 1223 K, quenched and reground after each of these steps. The crystal structure and the purity of the expected new phase were tested in the prepared samples by standard X-ray powder diffraction analyses. From these results $BiY_{0.65}R_{0.35}GeO_5$ for R = Pr and Nd, and stoichiometric

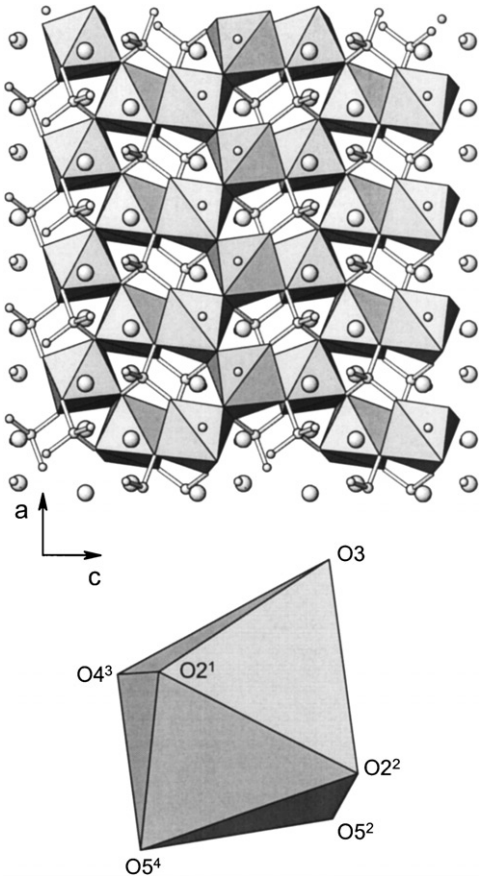

Fig. 1. View of the $(GeRO_5)_\infty$ layers along the (010) direction in the $BiRGeO_5$ structure. $(RO_7)_6$-units of edge sharing RO_7 polyhedra, the Ge (small spheres) in tetrahedral coordination, and the large spheres representing the position of Bi^{3+} cations, are shown, top. The RO_7 C_{2v} monocapped trigonal prism is displayed at the bottom.

samples for remaining *R* were finally prepared for subsequent spectroscopic studies.

For the stoichiometric Er sample the neutron powder diffraction NPD pattern was collected at room temperature on the D20 diffractometer, ILL-Grenoble, with a wavelength of 1.350 Å, in the angular range $5 \leqslant 2\theta \leqslant 100°$, in steps $\Delta 2\theta$ of 0.1°. The Rietveld method was used to refine the crystal structure, and the data were analyzed with the WinPLOTR program [11]. A pseudo-Voigt function was chosen to generate the line shape of the diffraction peaks. The background was fitted to a polynomial refinable function. Further details can be consulted elsewhere [12].

Optical absorption OA was recorded in a Varian 5E spectrophotometer. Continuous wave photoluminescence PL of $BiEuGeO_5$ was obtained with a tunable dye laser by exciting at 463 and 578 nm. The emission was analyzed with a Spex 340E spectrometer and detected with a cooled R928 Hamamatsu photomultiplier using a lock-in amplifier. The resolution for both OA and PL experiments was in the range 0.5–1.0 Å. The samples, consisting of dispersed $BiEuGeO_5$ powder in

KBr pellets, were cooled to 10 K using an He close-cycled cryostat connected to a suitable temperature controller.

4. Results

X-ray analyses of the prepared samples indicate that the studied phase appears pure for compositions with $x \leqslant 0.35$ for R = Pr or Nd, while for smaller R ions, Sm to Yb, it appears for any x content.

Table 1 includes the unit cell and atomic parameters for the stoichiometric $BiErGeO_5$ compound, determined from the refinement of NPD data at room temperature. The presence of $Er_2Ge_2O_7$ [13] was detected as a secondary crystalline phase, which was included and refined in the above multipattern refinement. Fig. 2 shows observed and calculated NPD profiles at room temperature for $BiErGeO_5$. Main interatomic distances for $BiErGeO_5$ are listed in Table 2.

OA and PL spectra of $BiEuGeO_5$ show a narrow single line corresponding to the $^5D_0 \leftrightarrow {}^7F_0$ transition, at 17214 cm^{-1}. This indicates that Eu^{3+} occupies a single crystallographic site in the host, and that the studied sample consists of the pure phase. Moreover, the number of emission lines observed for $^5D_0 \rightarrow {}^7F_J$ transitions indicates that the degeneracy of these ^7F_J states is completely lifted, that is, we can assign the spectrum to a site of C_{2v} or lower symmetry, in accordance with crystal data. Although transitions to $^7F_5$ levels are missing in the PL spectrum observed by exciting the $^5D_0$ level, the position of some of them has been established from the weak transitions which appear by exciting $^5D_2$ at 463 nm, see Fig. 3. Up to five $^7F_6$ levels have been observed in the 10 K near infrared OA spectrum. In this way the derived energy level scheme with 29 $^7F_{JM}$ levels has been used in the CF simulation. Further, sharp lines observed in the wavelength range of 390–530 nm have been attributed to transitions from $^7F_0$ to $^5L_6$, $^5D_3$, $^5D_2$ and $^5D_1$ levels. Table 3 summarizes the experimental energy position, E_o, derived from our OA and PL 10 K measurements.

Table 1
Unit cell parameters and atomic coordinates for $BiErGeO_5$, *Pbca* (No. 61), $Z = 8$, from D20 NPD, at room temperature

a (Å)			5.314(4)
b (Å)			15.176(9)
c (Å)			10.999(7)
V (Å^3)			887(1)
No. reflections			1646
No. points			1536
R_p			3.27
R_{Bragg}			6.44
R_f			3.02
(x, y, z) Er	0.012(4)	0.052(1)	0.360(2)
(x, y, z) Bi	0.947(3)	0.240(1)	0.152(2)
(x, y, z) Ge	0.002(4)	0.402(1)	0.406(1)
(x, y, z) O1	0.063(3)	0.302(2)	0.335(2)
(x, y, z) O2	0.293(5)	0.437(2)	0.447(2)
(x, y, z) O3	0.309(5)	0.128(2)	0.488(2)
(x, y, z) O4	0.265(5)	0.150(2)	0.237(2)
(x, y, z) O5	0.364(4)	0.486(2)	0.187(2)

Overall temperature factor: 0.18(2) Å^2.

5. Crystal-field analysis and simulation of the energy level schemes: discussion

The phenomenological crystal-field CF simulation of the Eu^{3+} energy level scheme can be accurately conducted on the strongly reduced basis of the $^7F_{JM}$ set alone, i.e., 49 $|SLJM_J\rangle$ levels [8,14]. The use of this truncation is enabled by two characteristics of the $4f^6$ configuration: firstly, the ^7F_J ($J = 0-6$) sextuplet is relatively well isolated from the rest of the configuration (about 12,000 cm^{-1} between $^7F_6$ and $^5D_0$), which renders the mixing of the wavefunctions negligible, and secondly, the CF operator mixes only the levels with the same multiplicity. Evidently, even with the J-mixing included, this basis does not take into account all interactions, as non-diagonal spin–orbit interactions that create small components of the ^5D_J levels into the ^7F_J wavefunctions. Therefore, "intermediate parameters" have to be introduced, one for each ^7F_J state, to overlap experimental and calculated barycenters.

The method used for calculating the energy levels of Eu^{3+} in its crystalline environment usually considers the single-particle CF theory. Following the formalism of Wybourne [9], the CF Hamiltonian is expressed as a sum of products of tensor operators $(C_q^k)_i$, with real B_q^k and complex S_q^k parameters as coefficients,

Table 2
Selected interatomic distances (Å) in $BiErGeO_5$

Er–O2^1	2.42(3)	Er–O4^3	2.24(3)	Bi–O1^6	2.25(2)	Ge–O1	1.73(3)
Er–O2^2	2.25(3)	Er–O5^2	2.29(3)	Bi–O3^6	2.41(3)	Ge–O2	1.71(4)
Er–O3	2.41(3)	Er–O5^4	2.25(3)	Bi–O4^5	2.37(3)	Ge–O3^1	1.62(3)
Er–O4	2.41(3)	Bi–O1^5	2.30(3)	Bi–O4^6	2.08(3)	Ge–O5^3	1.79(3)

Symmetry code: 1 $(x-1/2, 1/2-y, 1-z)$; 2 $(1/2-x, y-1/2, z)$; 3 $(x-1/2, y, 1/2-z)$; 4 $(-x, y-1/2, 1/2-z)$; 5 $(1+x, y, z)$; 6 $(1/2+x, y, 1/2-z)$.

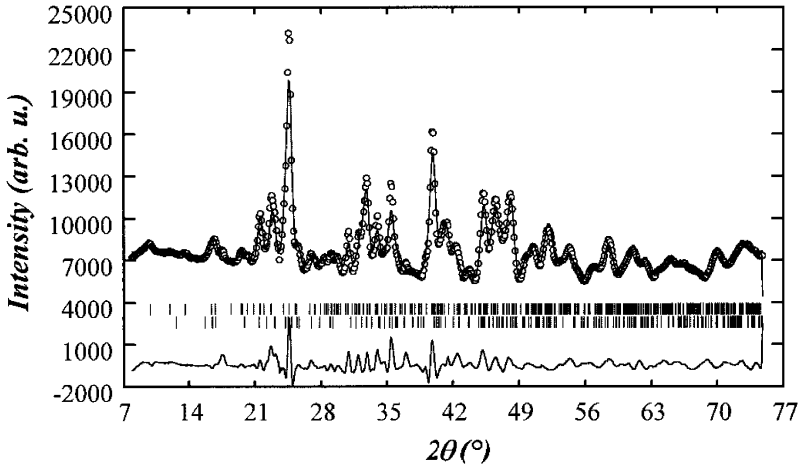

Fig. 2. Observed, calculated and difference neutron diffraction (D20, ILL-Grenoble) profiles of $BiErGeO_5$ at room temperature. Vertical marks correspond to the position of the allowed Bragg reflections for $BiErGeO_5$ (first row) and $Er_2Ge_2O_5$ (second row) structures. The difference curve is plotted at the bottom of the figure.

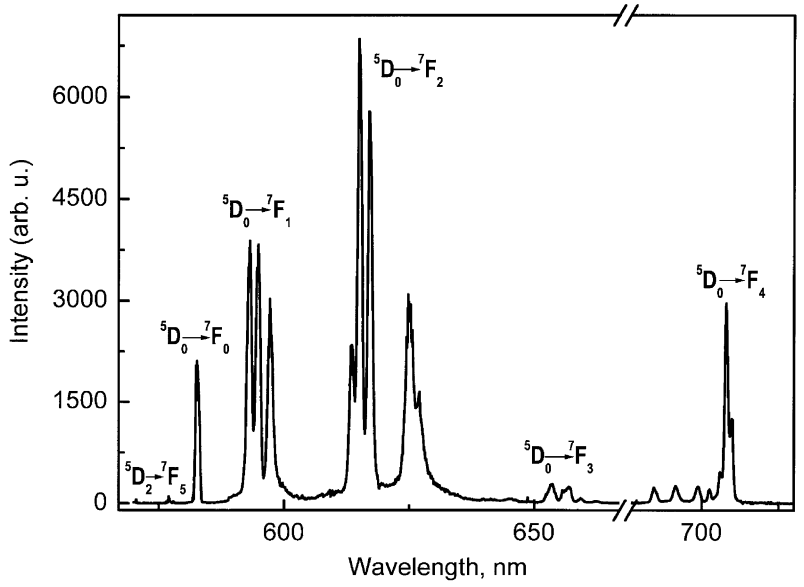

Fig. 3. Photoluminescence spectrum of $BiEuGeO_5$ at 10 K, $\lambda_{exc} = 463$ nm.

these later appropriated to the Eu^{3+} site symmetry in the host.

$$H_{CF} = \sum_{k=2}^{4,6}\sum_{q=0}^{k}\Big[B_q^k(C_q^k + (-1)^q C_{-q}^k) + iS_q^k(C_q^k - (-1)^q C_{-q}^k)\Big]. \quad (1)$$

For Eu^{3+} in $BiEuGeO_5$ the CF potential involves as many as 27 parameters, which obviously constitute non-realistic conditions for a simulation since the experimental data are not sufficient. Accordingly, we consider the approximate $C_2(C_s)$ symmetry, with 14 CF parameters. However, in order to make the simulation carefully, we carry out the descending symmetry procedure in several steps: (i) the first simulation is performed for the higher C_{2v} symmetry; accordingly, all S_q^k vanish, which gives nine CF parameters. In fact, following a previous planarity study [1], the shape of RO_7 in the host is defined as a C_{2v}-monocapped trigonal prism, giving us some crystallographic justification for this initial approach. (ii) The above nine CF parameters are considered as starting parameters for the simulation with the $C_2(C_s)$ symmetry, which now gives six additional non-zero S_q^k parameters, reduced to five by a proper choice of the reference axis system, canceling S_2^2. In each step, the refining procedure consists of making a three-phase calculation. The first one finds

Table 3
10 K observed (E_o) and calculated (E_c) in $C_2(C_s)$ symmetry energy levels (cm^{-1}) of Eu^{3+} in $BiEuGeO_5$[a]

$^{2S+1}L_J$	E_o	E_c	$^{2S+1}L_J$	E_o	E_c
$^7F_0$	0	0.3		—	4164
$^7F_1$	302	297		—	4178
	351	363		—	4193
	419	412		—	4201
$^7F_2$	869	859	$^7F_6$	—	4614
	909	917		—	4616
	964	968		—	4643
	1168	1170		—	4650
	1217	1215		—	4772
$^7F_3$	—	1875		—	4782
	1912	1914		4870	4867
	—	1940		4882	4872
	1963	1961		4924	4923
	1993	1996		4938	4934
	2046	2042		4979	4984
	2117	2116		—	4985
$^7F_4$	2611	2609	$^5D_0$	17214	
	2755	2754	$^5D_1$	18954	
	2904	2903		18967	
	—	2906	$^5D_2$	21376	
	2979	2981		21392	
	3050	3052		21429	
	3088	3088		21481	
	3124	3121	$^5D_3$, $^5L_6$	24769	
	3128	3129		24876	
$^7F_5$	—	3795		25045	
	—	3804		25141	
	—	3847		25279	
	—	3952		25304	
	4046	4044		25365	
	4073	4071		25392	
	—	4146		25405	

[a] The CF simulation includes only ^7F_J levels.

the B_q^2 sets reproducing the $^7F_1$ splitting. The second keeps B_q^2 fixed and includes the observed $^7F_2$ energy levels and the fourth-order B_q^4 parameters, in order to test their possible values, choosing then the best B_q^4 set from the smallest root mean squares rms deviation. Finally, B_q^6 parameters are calculated from the remaining levels, before considering all these observed levels and a free variation of all CF parameters.

The procedure is relatively involved, and trying to simplify it, a semi-empirical set of rough B_q^k and S_q^k parameters, estimated by a calculation from the Simple Overlap Model (SOM) [10], has been also used. In SOM it is assumed that the interaction energy of R^{3+} in its environment in the host is produced by an electrostatic potential created by charges uniformly distributed over small regions centered around the mid-point of the R_L distances from R^{3+} to the ligand, L. The charge in each region is proportional to the total overlap integral ρ between the $4f$ orbitals of R^{3+} and those of L. The two adjustable parameters required for the model were fixed to the standard values of -0.8 for the effective charge for the oxygen [15] and 0.057 for ρ [10]. Required crystallographic data are restricted to R^{3+} and its first coordination sphere of ligands [1].

Table 4
Phenomenological CF parameters for $BiEuGeO_5$

	C_{2v}	$C_2(C_s)$
B_0^2	340 (20)	324 (15)
B_2^2	122 (13)	164 (10)
B_0^4	−898 (33)	−982 (25)
B_2^4	162 (33)	18 (28)
S_2^4	—	434 (26)
B_4^4	−1163 (21)	−1096 (15)
S_4^4	—	85 (45)
B_0^6	615 (51)	329 (42)
B_2^6	643 (45)	561 (36)
S_2^6	—	−213 (22)
B_4^6	−753 (27)	−762 (23)
S_4^6	—	343 (48)
B_6^6	−566 (42)	−411 (42)
S_6^6	—	112 (38)
Levels	29	29
d_m	10.2	4.1
σ	12.3	5.6
Residue	3019.5	501.1

Values in parentheses are the estimated standard deviations. All values are in cm^{-1}.

Table 5
Comparison between SOM-calculated ($\rho = 0.057$) and experimental CF strength parameters (cm^{-1}) for $BiEuGeO_5$

	SOM (C_1)		CFexp (C_2/C_s)
S_2	225	S_2	178
S_4	664	S_4	646
S_6	411	S_6	446
S_T	469	S_T	465

The set of final phenomenological CF parameters is presented in Table 4. The sequence of experimentally observed energy levels is very well reproduced with CF parameters corresponding to the $C_2(C_s)$ symmetry, as it can be seen in Table 3.

Table 5 presents the comparison between phenomenological and SOM-calculated CF parameters, for the approximate $C_2(C_s)$ and for the true C_1 symmetries, respectively, which was made through the corresponding k-rank S_k and the total S_T CF strengths, defined as follows [16]:

$$S_k = \left\{ 1/(2k+1) \left[(B_0^k)^2 + 2 \sum_q \left[(B_q^k)^2 + (S_q^k)^2 \right] \right] \right\}^{1/2}, \quad (2)$$

$$S_T = \left[\frac{1}{3} \sum_k S_k^2 \right]^{1/2}. \quad (3)$$

SOM estimates very accurately the B_0^2 and B_2^2 parameters, 326 and 162 cm^{-1}, respectively, which are

the more sensitive to the magnitude of electrostatic short-range interactions, and all global S_k and S_T CF strengths. The values for other parameters, especially the S_q^k ones, are only poorly derived. We can reasonably think that the different symmetries considered in both phenomenological and semi-empirical methods are at the basis of these divergences. For C_1 SOM calculates 27 CF parameters whereas only 14 are involved in the CF potential of the $C_2(C_s)$ symmetry, and since CF S_k strengths are calculated from *absolute values* of the CF parameters corresponding to a given symmetry, in the later case individual parameters will be larger, always in absolute values, than in C_1.

On the other hand, when phenomenological C_{2v} and $C_2(C_s)$ parameters are compared it is clear that values of S_q^k parameters are not lower but comparable to most of the B_q^k ones. This means that in spite of the initial consideration of the C_{2v} symmetry for the RO_7 coordination polyhedron, as the previous work indicates [1], the crystal environment of the optical Eu^{3+} center in $BiEuGeO_5$ is rather more distorted.

The difficulty to assure a CF calculation for an R ion in a low point-group symmetry, which is mainly derived of the large number of adjustable parameters required to fit the experimental data with a total Hamiltonian, is a well-known fact [17]. A number of minima may exist that are indistinguishable from the point of view of the quality of the fit. In order to settle the problem, several ways described [17] in the literature have been now explored in the search for a reliable minimum. First, because imposing theoretical constraints can alleviate these difficulties, SOM has been chosen among the various theoretical models [18] describing CF interactions. It has allowed an easy initial evaluation of CF parameters. Further, the consideration of a higher, but close to the true, symmetry has been also tested [9]. Finally, the more secure way for operating such a simulation is to perform simultaneously the same calculation for other R configurations in the same matrix [19], up to obtain a smooth evolution of individual CF parameters along the isostructural R series. In the current CF analysis, the consistency found between $C_2(C_s)$ phenomenological and C_1 SOM-calculated CF strength parameters, along with the excellent agreement between the experimental and the $C_2(C_s)$ simulated energy level schemes, and very especially the similar values of CF parameters obtained from simulations performed for the remaining $4f^N$ configurations, which include adequate free-ion parameters, in the same $BiRGeO_5$ host [20], are indications of the reliability of the followed process and results.

Acknowledgments

The authors acknowledge the financial support of the Spanish MCyTMAT2002-04603-C05-05 and MAT2001-1433 projects, and the Institut Laue Langevin for neutron scattering facilities offered.

References

[1] C. Cascales, J.A. Campá, E. Gutiérrez Puebla, M.A. Monge, C. Ruíz Valero, I. Rasines, J. Mater. Chem. 12 (2002) 3626.
[2] B. Aurivillius, C.I. Lindblom, P. Stenson, Acta Chim. Scand. 18 (1964) 1555.
[3] A. Yu Shaskov, V.A. Efremov, A.A. Bush, N.V. Rannev, Yu.N. Venevtsev, V.K. Trunov, Zh. Neorg. Khim. 31 (1986) 1391.
[4] C. Sussieck-Fornefeld, Heidelberg geowissenschaftliche Abhandlugen 17 (1988) 139.
[5] A.G. Vidgorchik, L.N. Dem'yanets, Yu.A. Malinovskii, Kristallografiya 32 (1987) 1381.
[6] K. Kato, M. Sekita, K. Shigeyuki, Acta Crystallogr. B 35 (1979) 2201.
[7] L. Brixner, J. Calabrese, H.Y. Chen, J. Less-Common Met. 110 (1985) 397.
[8] P. Porcher, P. Caro, J. Chem. Phys. 65 (1976) 89.
[9] B.G. Wybourne, Spectroscopic Properties of Rare-earths, Wiley, New York, 1965.
[10] P. Porcher, M. Couto dos Santos, O. Malta, Phys. Chem. Chem. Phys. 1 (1999) 397.
[11] T. Roisnel, J. Rodríguez Carvajal, WinPLOTR Program for Rietveld Refinement and Pattern Matching Analysis, Laboratoire Léon Brillouin, CEA-CNRS, Centre d'Etudes de Saclay, France, 1999.
[12] C. Cascales, M.T. Fernández Díaz, M.A. Monge, Chem Mater. 12 (2000) 3369.
[13] Y.I. Smolin, Kristallografiya 15 (1970) 47, PDF # 720745, PCPDFWIN 2.2, 2001, JCPDS-ICDD.
[14] C. Cascales, P. Porcher, J. Fernández, A. Oleaga, R. Balda, E. Diéguez, J. Alloys Compd. 323–324 (2001) 260.
[15] C.A. Morrison, R.P. Leavitt, Spectroscopic properties of triply ionized lanthanides in transparent host crystals, in: K.A. Gschneidner Jr., L. Eyring (Eds.), Handbook on the Physics and Chemistry of Rare Earths, Vol. 5, North-Holland, Amsterdam, 1996.
[16] N.C. Chang, J.B. Gruber, R.P. Leavitt, C.A. Morrison, J. Chem. Phys. 76 (1982) 3877.
[17] C. Görller-Walrand, K. Binnemans, Rationalization of crystal-field parametrization, in: K.A. Gschneidner Jr., L. Eyring (Eds.), Handbook on the Physics and Chemistry of Rare Earths, Vol. 23, North-Holland, Amsterdam, 1996.
[18] D. Garcia, M. Faucher, Crystal field in non-metallic (rare earth) compounds, in: K.A. Gschneidner Jr., L. Eyring (Eds.), Handbook on the Physics and Chemistry of Rare Earths, Vol. 21, North-Holland, Amsterdam, 1995.
[19] J. Hölsa, R.J. Lamminmäki, J. Lumin. 69 (1996) 311.
[20] C. Cascales, C. Zaldo, unpublished.